

Processing and interpretation of 3C-3D seismic data: Clastic and carbonate numerical models

Glenn A. Larson¹ and Robert R. Stewart

ABSTRACT

Three-dimensional (3-D) seismic images have become an essential tool in seismic exploration. The interpretation tools and practices for conventional (acoustic) 3-D have been developed over the past 20 years. Converted-wave seismic images can accompany a conventional acoustic survey and provide a powerful adjunct to a more complete interpretation. A 3-D converted-wave survey is acquired using a numerical model. The model contains a clastic and a carbonate setting. Extra elastic-wave information (e.g. Vp/Vs values, P-P and P-S amplitude maps) allows further characterization of the clastic anomaly. The elastic-wave data successfully identifies a thickening wedge of porosity at the top of the reef in the carbonate model.

INTRODUCTION

The goal of this paper is to implement P-S interpretation techniques in a 3-D geometry. Modelling can anticipate effects in real data by making various assumptions or parameter changes in the synthetic case (Sheriff, 1991). Numerical modelling is useful in understanding and anticipating problems in field acquisition design, seismic processing, and interpretation. This is especially important before entering into an expensive field program.

Interpretation techniques for converted-wave seismic data have been previously developed in the 2-D realm. At Carrot Creek, Alberta, Nazar (1991) and Harrison (1992) implement the techniques of S1 and S2 polarization separation, P-S and P-P AVO analysis, Vp/Vs ratios, and amplitude analysis for a 2-D converted-wave dataset. Miller et al. (1994) interpret 2-D converted-wave seismic from the Lousana Field in central Alberta. P-P and P-S synthetics are correlated with the field data, and Vp/Vs ratios are profiled in order to characterize a Nisku target.

3-D interpretation of conventional P-P seismic data have also been well established (e.g. Brown, 1991). Concepts such as *mapping* of attributes and structure, time slice development, 3-D visualization, and 3-D AVO have become routine practices. Al-Bastaki et al. (1994) characterize a carbonate target using a 3-D shear-source dataset. 3-D interpretation techniques can now be applied to converted-waves. This paper will enhance the converted-wave interpretation techniques previously developed in 2-D. We will integrate 3-D attribute *mapping* from converted-wave seismic data with the conventional seismic volume that is acquired with the same source effort.

¹ Amoco Canada Petroleum Company Ltd., 240 - 4th Avenue SW, Calgary, Alberta.

MODEL DESCRIPTION

Clastic Model

The clastic model is based upon the Viking formation in central Alberta. The Viking sand P-wave velocities (V_p) are similar to the surrounding shales in the Western Canada Sedimentary Basin (Schaffer, 1993) and make conventional seismic exploration difficult. V_p and formation thicknesses are taken from the 10-22-39-26W4 well and modelled after a Viking oil field over sections 4 to 6 in Township 39, Range 26W4. Nazar (1991) provides shear-wave velocities (V_s) in the Mesozoic section from the Carrot Creek field northwest of the study area. The V_s of the Viking sandstone is determined from an array sonic log at 9-5-39-3W5 over the Medicine River Field.

Three sandstone channels are constructed in the MIMIC geologic modelling system (from Western Geophysical, Inc.). The inscribed channels are described by two half-ellipsoids and one hemisphere of thicknesses ranging from 15 to 25m, which are typical thicknesses for producing Viking fields in the area (Leckie et al., 1994). A plan view of the Viking bodies are shown in Figure 1. A cross section is shown in Figure 2. Table 1 describes the layer velocities and thicknesses.

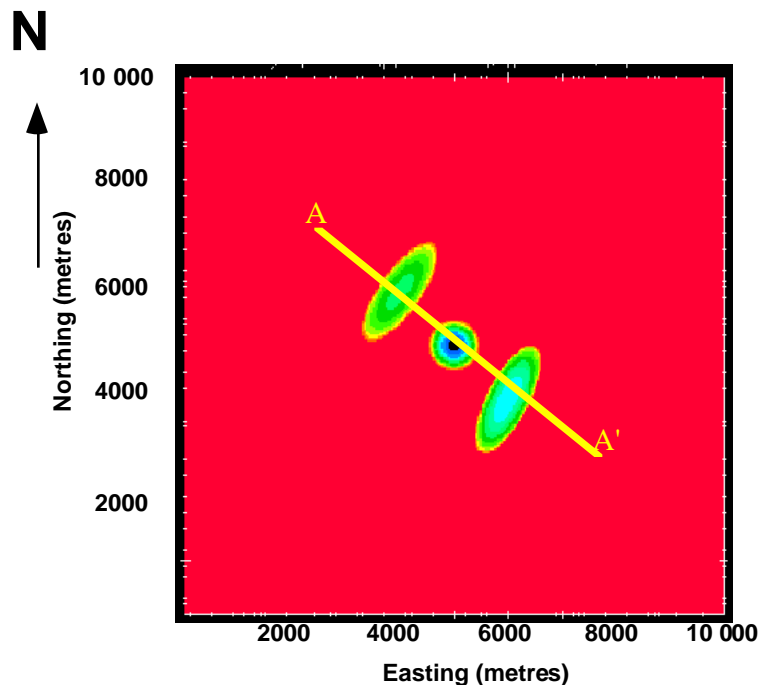


Figure 1: Plan view of clastic model. The thicknesses of the bodies range, from northwest to southeast: 15m, 25m, and 20m, respectively. The A-A' cross-section marker refer to Figure 2.

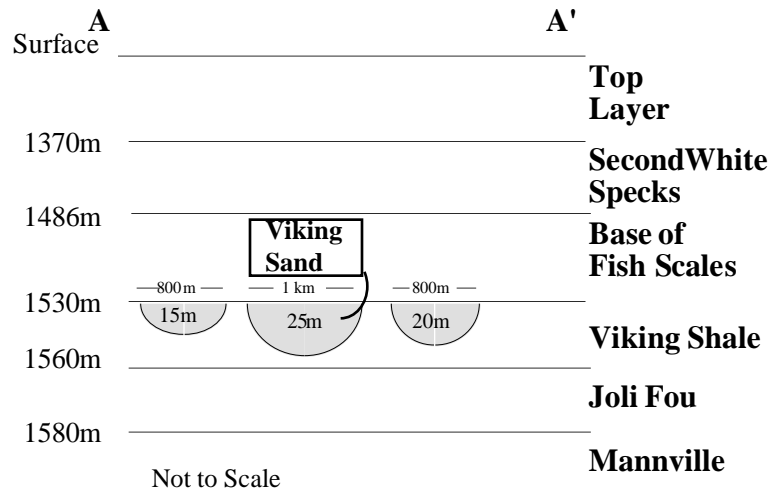


Figure 2: Cross-section of clastic model.

Layer	Depth(m)	Vp(m/s)	Vs(m/s)	Vp/Vs
Top Layer	0	3500	1750	1.87
Second White Specks (2WS)	1370	3350	1876	1.79
Base of Fish Scales (BFS)	1486	3280	1574	2.08
Viking Sand	1530	4166	2541	1.64
Viking Shale	1530	4000	2000	2.0
Joli Fou	1560	2771	1330	2.08
Mannville	1580	4100	2457	1.7

Table 1: Clastic model layer velocities and thicknesses

Carbonate model

The carbonate model is a stratigraphic trap consisting of a shelf transition from dolomite to shale. The thicknesses and Vp values for the Wabamun, Nisku, and Ireton are taken from the 10-22-39-26W4 well. The Vs values are calculated from Vp/Vs values taken from the Miller et al. (1994) study of the Lousana field southeast of the 10-22-39-26W4 location.

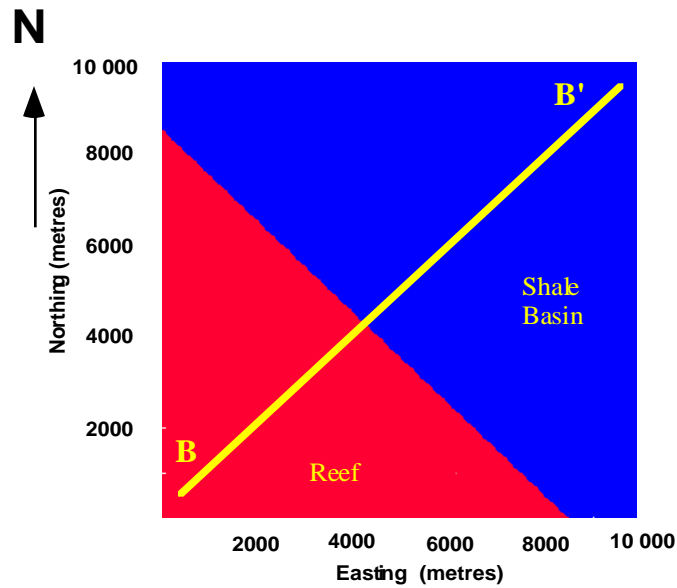


Figure 3: Plan view of carbonate model. The B-B' cross-section is shown in Figure 4.

The model consists of 7 layers. Figure 3 and 4 show the model in plan view and cross-section, respectively. Encased within the reef is a wedge of dolomite porosity. The porosity wedge increases in thickness from 8 to 32m across from the southeast to the northwest areas of the reef. Table 2 describes the layer values.

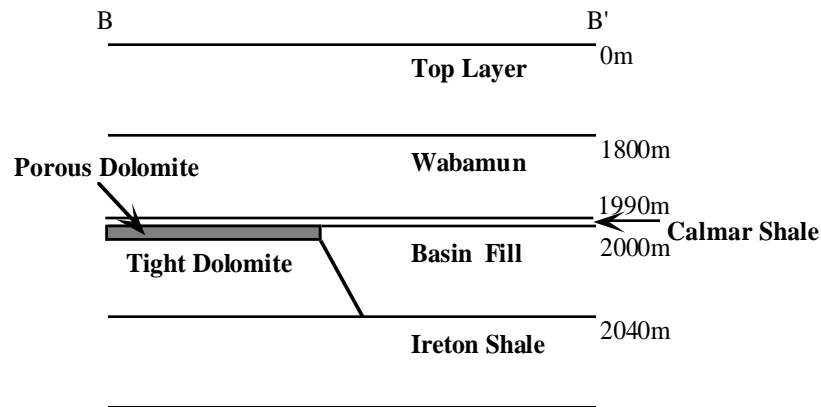


Figure 4: Cross-section of carbonate model

Layer	Depth(m)	Vp(m/s)	Vs(m/s)	Vp/Vs
Top Layer	0	3480	1740	2.0
Wabamun	1800	5995	3177	1.9
Calmar Shale	1990	5400	2592	2.1
Porous Dolomite	2000	5340	3043	1.75
Basin Fill	2000	6400	3200	2.0
Tight Dolomite	2008-2032	7090	3970	1.8
Ireton	2040	5500	2640	2.1

Table 2: Carbonate model velocities and thicknesses

DATA ACQUISITION

Raytracing of the two models are completed on Sierra's 3-dimensional QUIKSHT offset raytracing package, which provides shot record simulations. The software uses a WKBJ raytracing technique for amplitude determination. Ray instructions are defined for each layer interface, and is flexible enough to generate converted-waves. The raytracing uses a straight-line technique between each layer and follows Snell's Law for travel time estimates.

Acquisition design

The same design parameters are used for both models. The design is based upon the 3-D P-P and P-S design criteria described in Lawton (1994). Table 3 summarizes the survey parameters. The desired bin size for the survey is 50m x 50m. This results in a shot and receiver spacing of 100m. The coverage of the targets requires a 5600 x 5000m survey. The offset range, based upon the minimum and maximum depths of the two models, are 900 and 3000m, respectively.

The most important P-S design criterion is the prevention of empty CCP bins. Gaps in CCP fold can be mitigated by decreasing the shot line interval to 500m, an odd integer multiple of the receiver spacing, from its original CMP design of 600m. This will prevent the imposition of empty bins and high fold periodicity that can occur if the design was based solely upon CMP considerations. Lawton et al. (1995, *this volume*) further develop 3-D CCP design by using the flexi-bin approach.

Shot Spacing (SI) = 100m (56 shots/line)
Receiver Spacing (RI) = 100m (52 receivers/ line)

Shot Line Interval (SL)= 500m* (11 lines)
Receiver Line Interval (RL) = 800m (8 lines)

Recording Template: All receivers live
Bin Size = 50 x 50m

Offset Range: 0 - 7000m

Maximum P-P Fold: 44
Maximum P-S Fold: 26
(0 - 2600m mute)

Total Number of Traces for each mode of recording: 240 000

* Odd multiple of receiver spacing

Table 3: 3C-3D Recording Parameters

The receiver line increment (RL) defines the largest minimum offset. To image the shallowest layer at 900m, an RL of 800m is chosen. All 8 receiver lines, consisting of 416 receivers, were left live for each of the 616 shots (Figure 5). The receiver patch size allows far offsets to extend to 7000m. A receiver template of this size is unnecessary for targets at this depth, but the modelling software is inflexible in describing the movement of smaller receiver templates. For simplification, all receivers are left on for each shot and the long offsets are muted in processing.

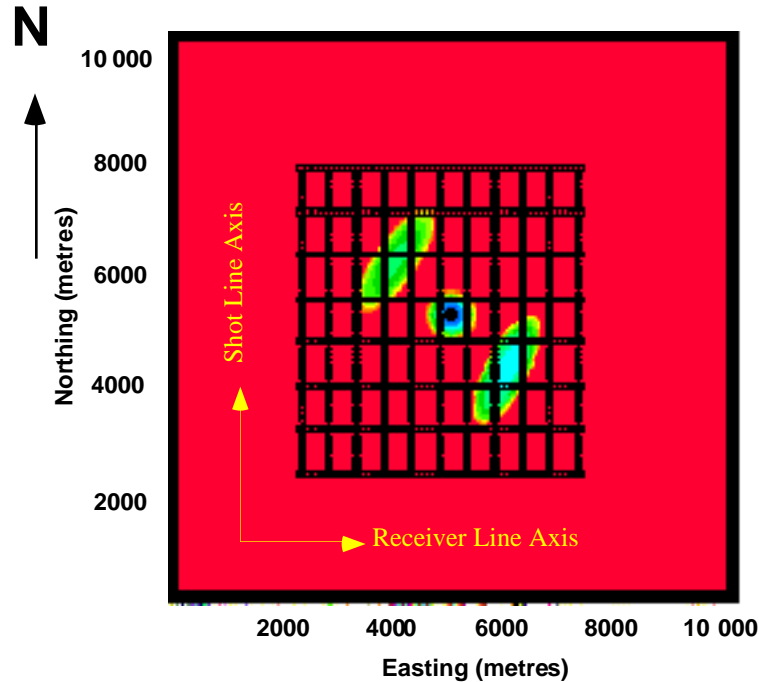


Figure 5: Shot and receiver grid (shown over the clastic model).

Figures 6 and 7 display the CMP and CCP fold distribution for 0-2600m offsets. P-P and P-S fold maps for a shot line interval of 600m (an even multiple of RI) are shown in Figure 8. The fold periodicity of the P-S design (Figure 7) is smoother than a design with an even shotline integer spacing. An optimal bin size of 66.6m would smooth the P-S fold, but the bin sizes of the CMP and CCP data volumes should be kept the same for a consistent interpretation (Lawton, 1994).

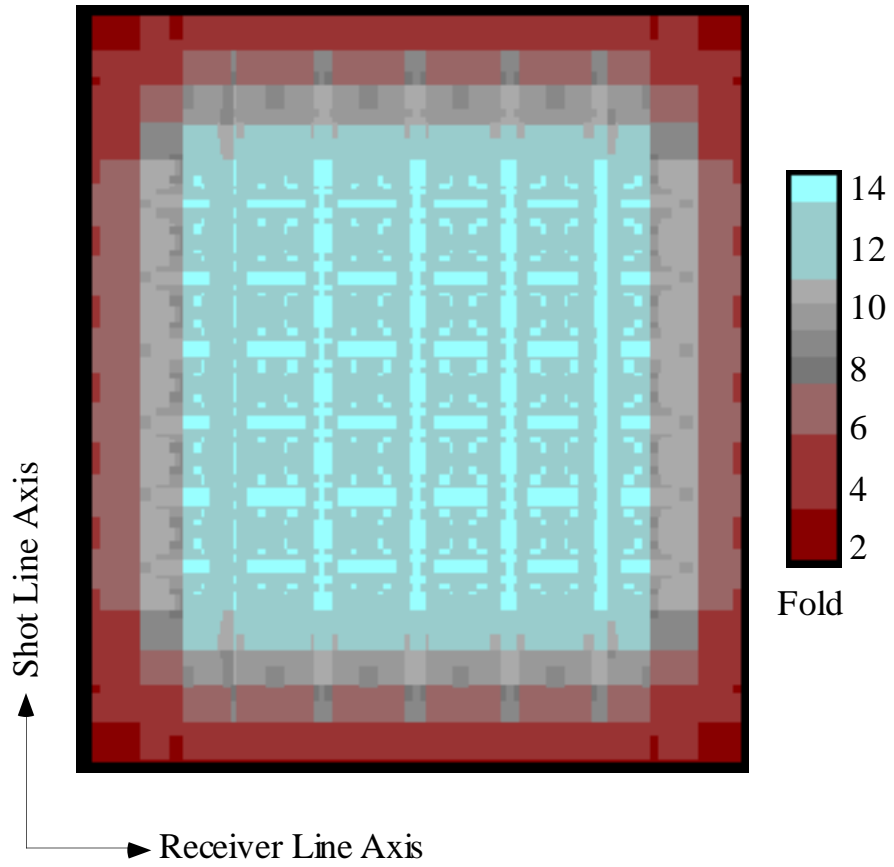


Figure 6: P-P model fold map. Offset range: 0-2600m. Bin size = 50m x 50m. Fold map dimensions = 5200m x 5600m.

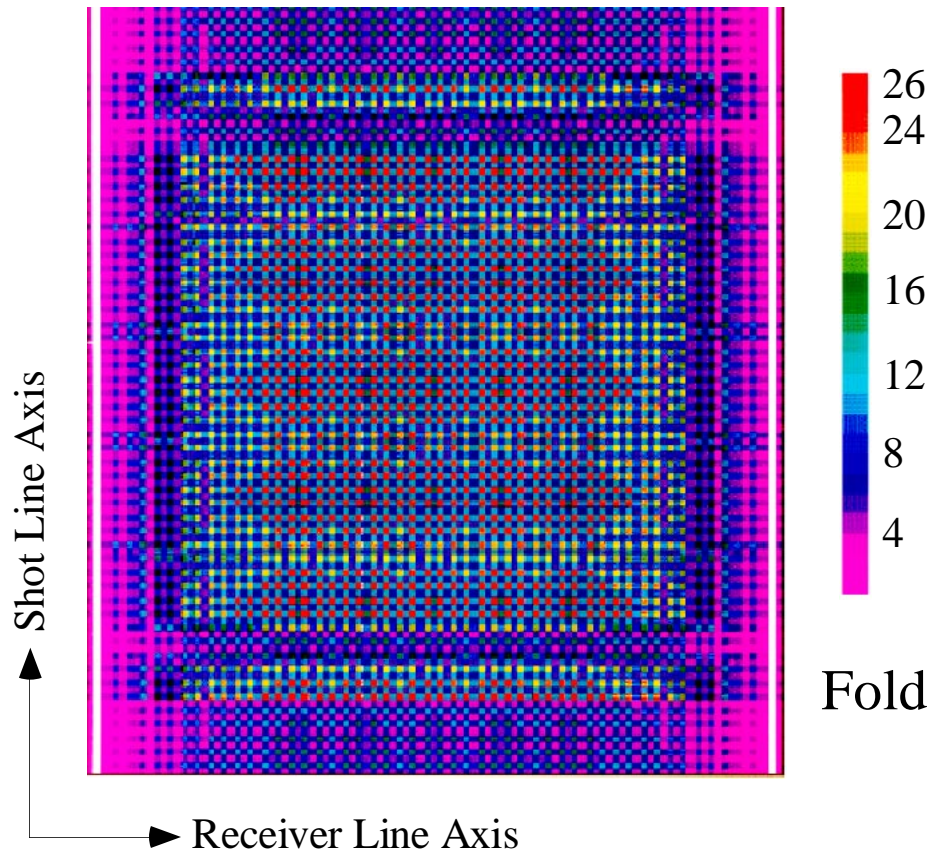


Figure 7: P-S numerical model fold map. Offset range: 0-2600m. Bin size = 50m x 50m. Fold map dimensions = 5200m x 5600m.

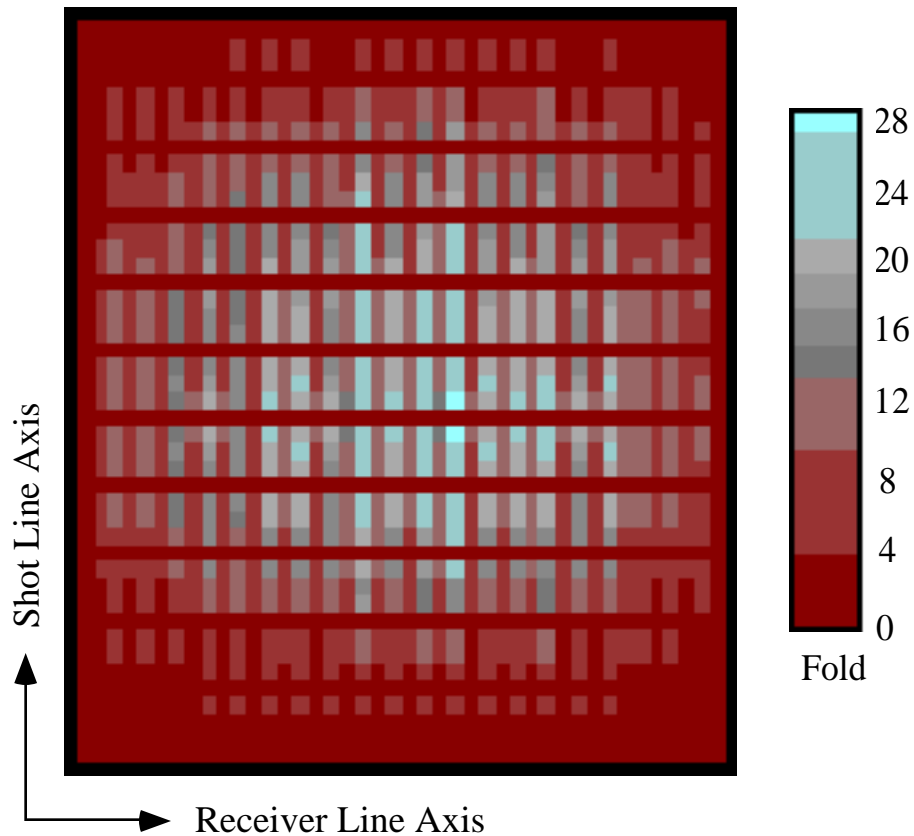


Figure 8: P-S fold map for a shot line spacing of 600m (even integer of the receiver spacing). Note the fold gaps with this increment of shot line spacing. Fold map dimensions = 5200m x 5600m.

Steps in acquisition

Figure 9 displays the steps required for the numerical model acquisition. The acquisition uses 3 separate Sierra modules: MIMIC (model construction), QUIKSHT (raytracing), and SLIPR (reformatting, convolution, and SEG Y output). The geologic model constructed within the MIMIC module is transferred to the QUIKSHT module. Within QUIKSHT, the source and receiver grids are built. The survey is acquired twice for each model: Once for P-P ray instructions and once for the P-S ray instructions. SLIPR reformats and convolves the raytracing information into SEG Y format for processing.

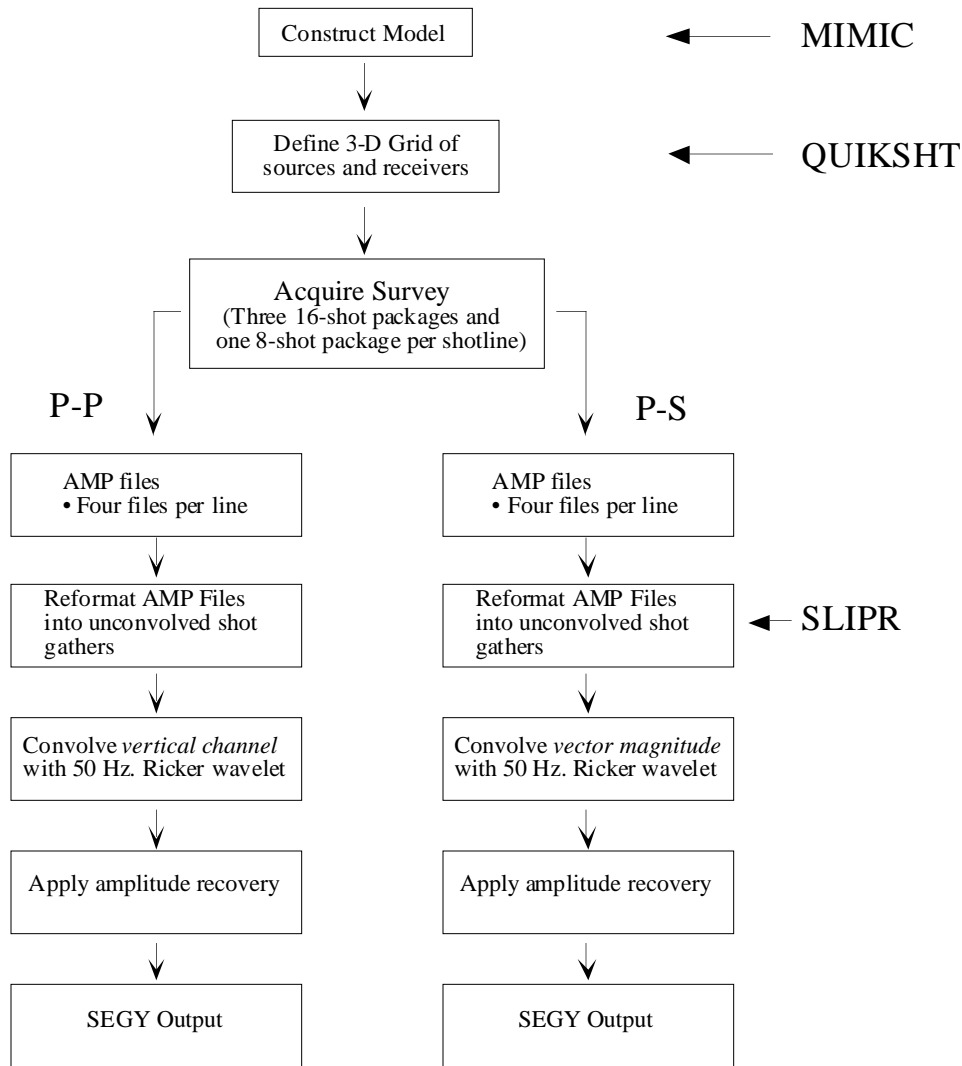


Figure 9: Acquisition steps of a 3-D numerical model for Sierra raytracing software.

Raytracing

Amplitude (AMP) files are created during a QUIKSHT raytracing run. For each shot the rays are captured by the receiver grid. The ray interaction at each layer is controlled by the ray instruction. The AMP files store the captured ray's travel time, amplitude, and the ray instruction for each layer. Two separate raytracing runs are performed with the P-P ray instructions and then again for the P-S ray instructions. Disk size and internal software limitations prevent the survey from being acquired at once. Internal memory constraints imposed by the Sierra system limit the size of an AMP file to 16 Megabytes. Because of this constraint, only 16 shots can be stored per AMP file. To accommodate the large size of the survey, each shot line is separated into three 16-shot groups and one 8-shot group. 44 AMP files are created for each full survey.

Reformatting and convolution

The SLIPR module reformats each AMP file into 32 unconvolved receiver gathers (EDD files). The spike seismograms are convolved with a 50 Hertz Ricker wavelet.

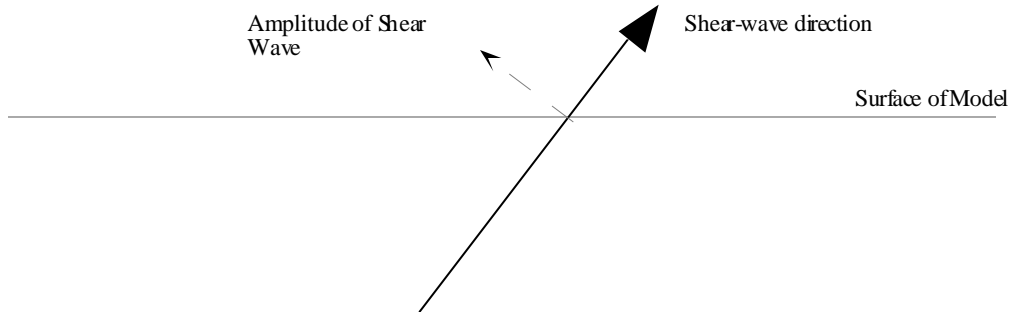


Figure 10: Vector amplitude of the incoming shear-wave raypath upon the Sierra system. This amplitude is recorded and convolved with the wavelet.

The convolution is done with the vertical receiver component for the P-P data and the total vector displacement (Figure 10) for the P-S. The vector displacement is the amplitude of the shear wave perpendicular to the incoming ray at the measuring surface. This method is used for several reasons:

- 1) The data are recorded on only one channel. This lowers the disk space demands by one-half.
- 2) It effectively completes the radial-transverse rotation that is required if the data were recorded on two orthogonal channels (Lane and Lawton, 1993). The model is isotropic so all the energy is expected to be on the radial channel.
- 3) The model lacks a low velocity near surface layer that would refract the incoming ray direction to vertical. The vector magnitude removes P-P leakage onto the horizontal channels.

Geometric spreading amplitude recovery is applied at the convolution step. 128 SEG Y files per shotline are created. These files are imported into ProMax for processing.

PROCESSING

Pre-processing

Prior to geometry assignment, the individual shot line SEG-Y files are combined into a full 3-D survey. The final Sierra output presents 1408 separate SEG-Y files each for the P-P and P-S surveys. Each file consists of 16 or 8 shot gathers sorted for each receiver line. To create one large file suitable for 3-D processing the following steps are taken:

- 1) The SEG-Y files are input by shot line. For each shot line, the FFID (field file identification number) header words are renumbered sequentially.
- 2) The shotlines are sorted by FFID and channel number. Each new shotline ensemble is written and merged together to form 56 shot gathers consisting of 416 receivers.
- 3) Repeat steps 1 and 2 for the remaining shot lines.

3-D P-P processing

The processing flow for the P-P data is shown in Figure 11. Figure 12 displays a typical shot record for the survey. After pre-processing and geometry assignment, a velocity analysis is completed. Because of the simplicity of the model, a single velocity function is used. NMO and a 30% stretch mute is applied, followed by a stack and a 2-pass 3-D f-k migration. The data, consisting of 102 inlines and 112 crosslines, are loaded onto the LandMark Seisworks® for interpretation.

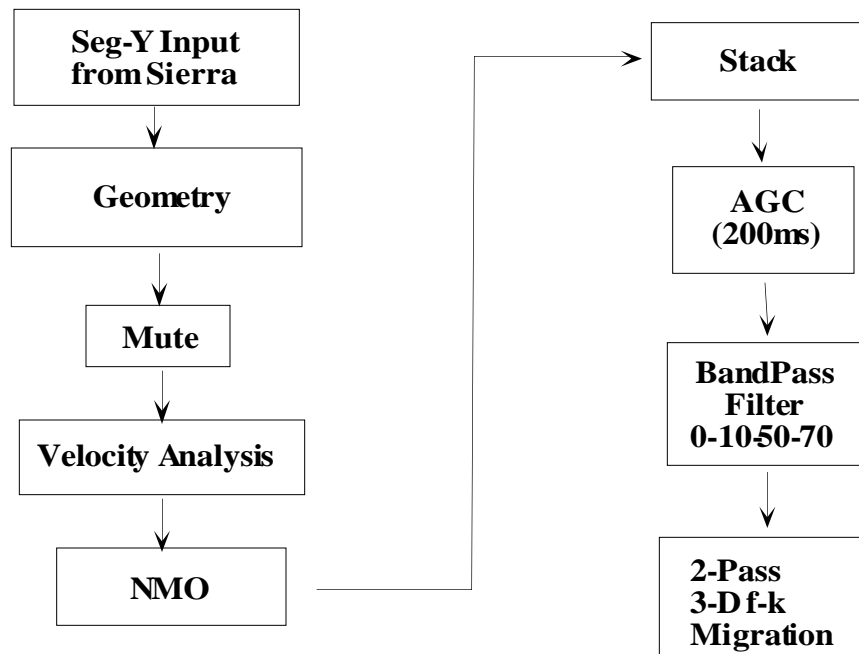


Figure 11: 3-D P-P processing flow.

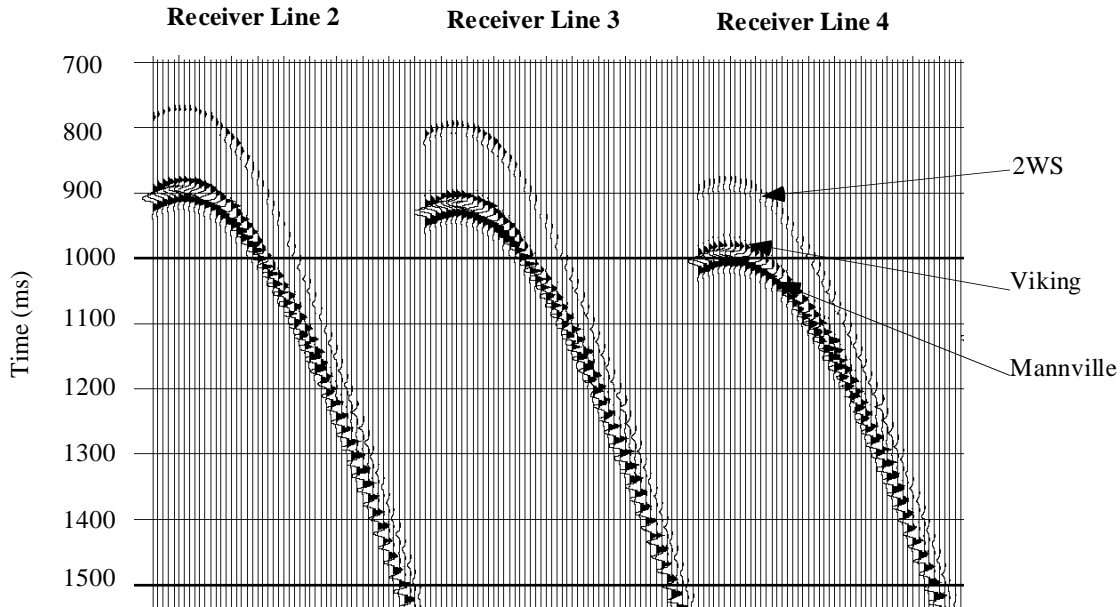


Figure 12: Shot record 47 of clastic P-P model.

3-D P-S processing

A general processing flow for 3-D converted-wave data has been developed by Cary (1994). The P-S processing flow is shown in Figure 13, and a typical P-S shot record is shown in Figure 14. The flow is similar to the P-P flow except for the addition step of binning by CCP location rather than CMP. The binning is completed in ProMax by header word manipulation. The new CCP locations are calculated using the asymptotic approximation (Harrison, 1992):

$$X_{\text{ccp}} = \frac{X_{\text{S-R}}}{1 + \frac{V_s}{V_p}}, \quad (1)$$

where X_{ccp} = distance of CCP point relative to the source location

$X_{\text{S-R}}$ = source-receiver offset

V_s = shear wave velocity

V_p = compressional wave velocity.

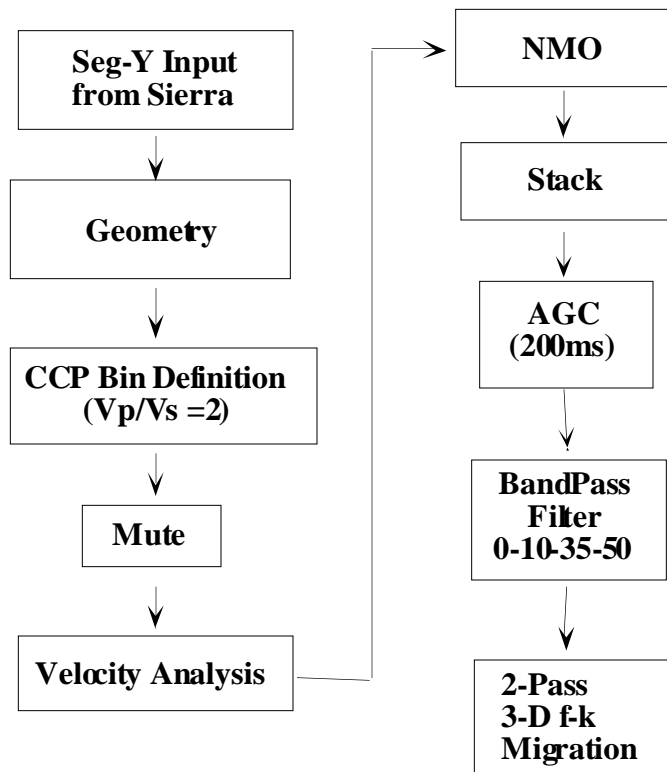


Figure 13: 3-D P-S processing flow.

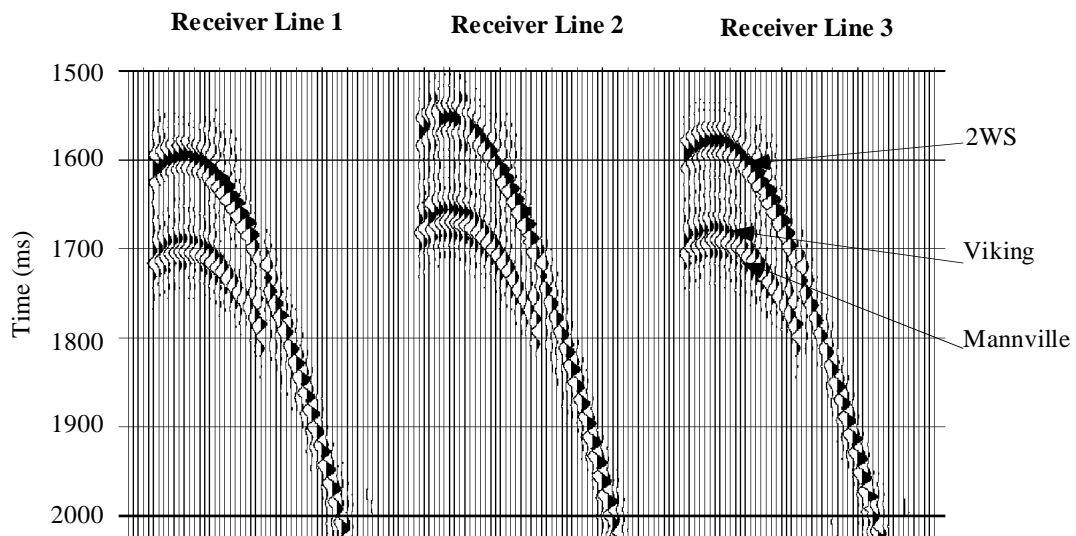


Figure 14: Record of shot 47 of 3-D P-S clastic model survey.

The data are re-binned at 50m bin sizes using the new CCP coordinates from the following equations:

$$\text{XLINE} = \left[\frac{\text{XCCP} - \text{X}_{\text{or}} + \frac{b_x}{2}}{b_x} \right] + 1, \quad (2)$$

where XLINE = crossline number

XCCP = asymptotic common conversion point X coordinate of trace

X_{or} = origin of X coordinate of survey coverage

b_x = bin size in x direction;

$$\text{ILINE} = \left[\frac{\text{YCCP} - \text{Y}_{\text{or}} + \frac{b_y}{2}}{b_y} \right] + 1, \quad (3)$$

where ILINE = cross line number

YCCP = asymptotic common conversion point X coordinate of trace

Y_{or} = origin of Y coordinate of survey coverage

b_y = bin size in y direction,

The CCP bins are given unique bin numbers by combining the ILINE and XLINE CCP flags:

$$\text{BIN} = \text{ILINE} * 1000 + \text{XLINE}, \quad (4)$$

where BIN = CCP bin number

ILINE = CCP in line number

XLINE = CCP cross line number.

The trace header values of CDP_X, CDP_Y, and the CDP bin numbers are replaced with the corresponding CCP values. With this replacement, converted-wave velocity analysis, stacking, and migration are completed with the standard CMP processes within ProMax.

The NMO correction does not incorporate the improved P-S NMO correction of Slotboom (1992) because of the high offset-to-depth ratio and because the correction has yet to be implemented in the ProMax processing system. A 10-20-35-50 Ormsby zero phase bandpass filter is applied to the P-S data. The filter lowers the bandwidth with respect to the P-P volume (0-10-50-60 Ormsby filter) to anticipate a lower field response for shear data. For the deeper carbonate model, the P-S volume is filtered somewhat lower with a 0-20-35-40 Ormsby bandpass filter. This is done to anticipate a reduction in frequency bandwidth at greater depth (Miller et al, 1994). The P-S stack is migrated with 95% of the RMS velocities from the velocity analysis (Harrison and Stewart, 1993). The migration is a 2-pass 3-D f-k method.

INTERPRETATION

Clastic model interpretation

The P-P and P-S volumes for the clastic model are loaded on the Landmark interpretation system. The event correlations along inline 54 of the P-P volume and the P-S volume are shown in Figures 15 and 16, respectively. The apparent polarity shift of the Second White Specks event is the result of a V_s increase rather than a V_p decrease. The Viking event on the P-P volume does not change. The P-S Viking event, however, is quite noticeable because of the increased V_s contrast between it and the BFS shale. There is also an amplitude reduction in the Mannville reflection below the Viking sand. The position of these anomalies correspond to the location of the sand bodies in the model.

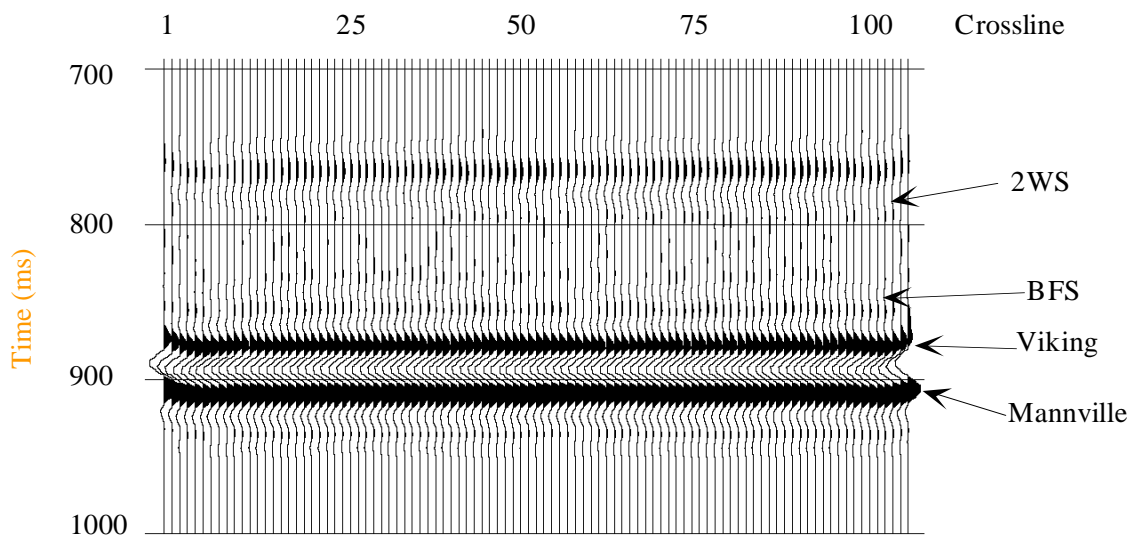


Figure 15: Inline 54 of the clastic model: P-P migrated volume.

The V_p/V_s ratios are calculated using the following equation (Harrison, 1992):

$$\frac{V_p}{V_s} = \frac{2 I_s}{I_p} - 1, \quad (5)$$

where I_s = time interval between two P-S reflections and
 I_p = time interval between two P-P reflections from the same reflector.

This equation is used to calculate V_p/V_s for the BFS-to-Mannville interval. Since the bin sizes are the same for both data volumes, the V_p/V_s can be directly calculated for every trace. As a result, 2-D converted-wave interpretative tools such as the V_p/V_s ratio (e.g. Nazar, 1991, Schaffer, 1993, and Miller et al., 1994) can be extended in 3-D by *mapping* this ratio for a given interval. The V_p/V_s map of the BFS to Mannville interval (Figure 17) clearly shows a relative reduction in the V_p/V_s ratios relative to the surrounding volume. The position of the sand anomaly is further accentuated by the maps of the Viking shear amplitude (Figure 18), the Mannville shear amplitude (Figure 19). The acoustic Viking amplitude (Figure 20) is very subtle, but when complemented by the P-S interpretive results, the position and identification of the sand bodies become more compelling.

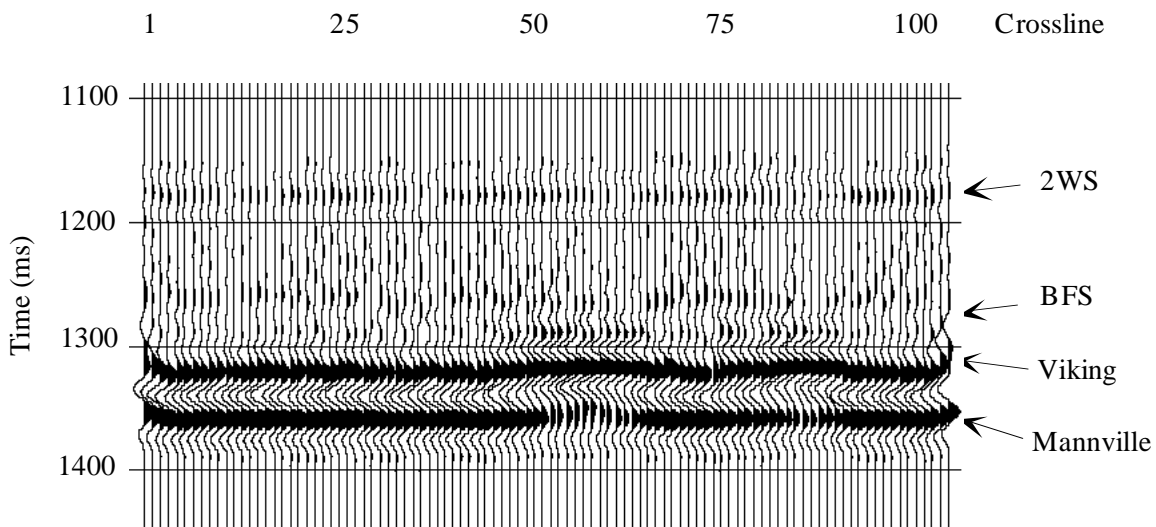


Figure 16: Inline 54 of the clastic model: P-S migrated volume.

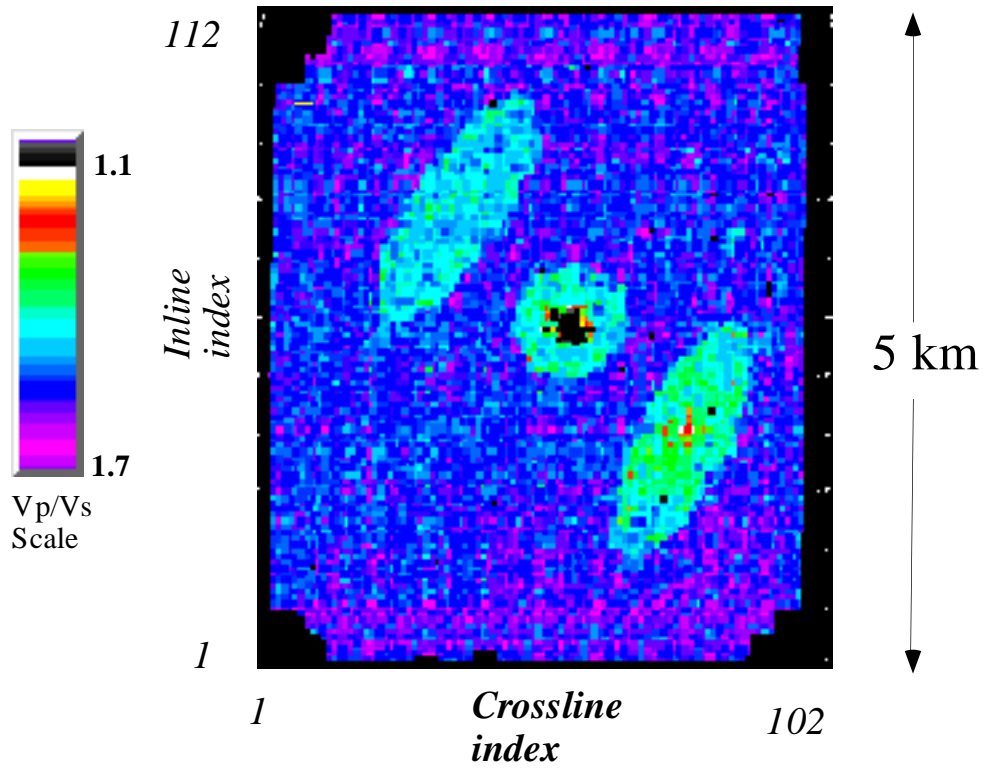


Figure 17: Vp/Vs map: Clastic model. Base of Fish Scales to Mannville interval.

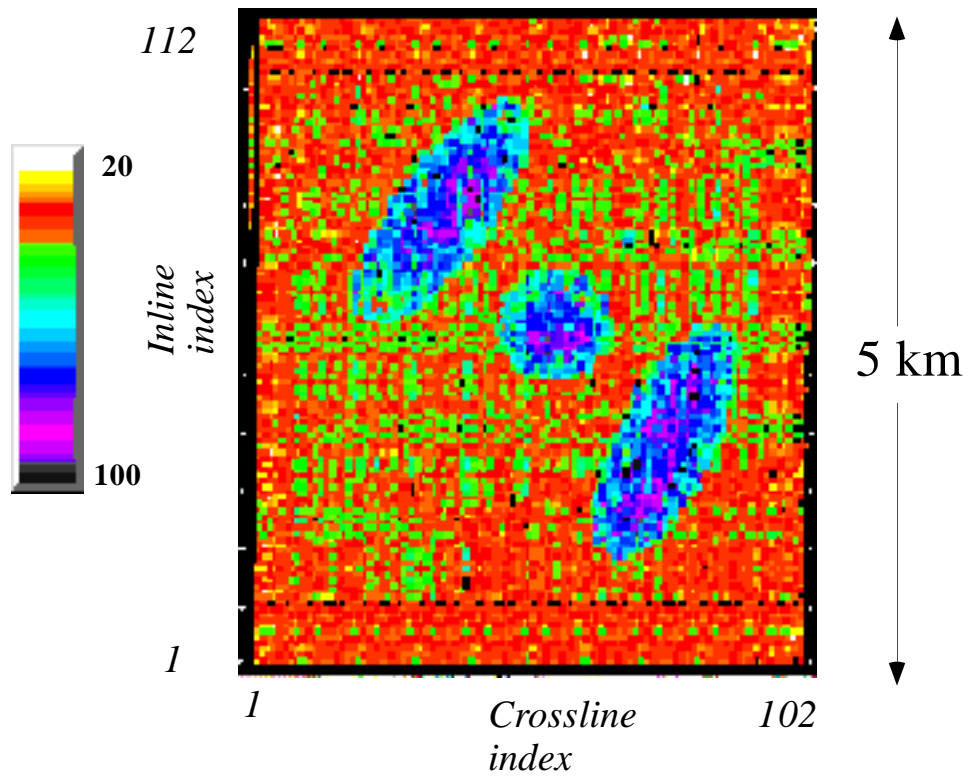


Figure 18: Viking shear amplitude map: Clastic model.

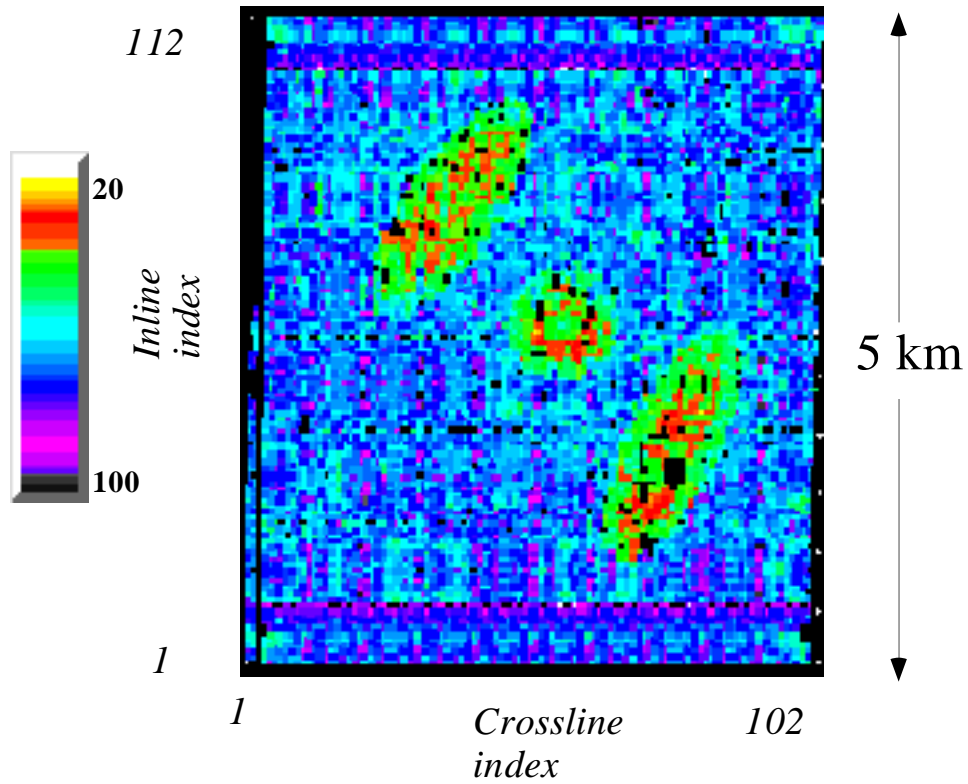


Figure 19: Mannville shear amplitude map: Clastic model.

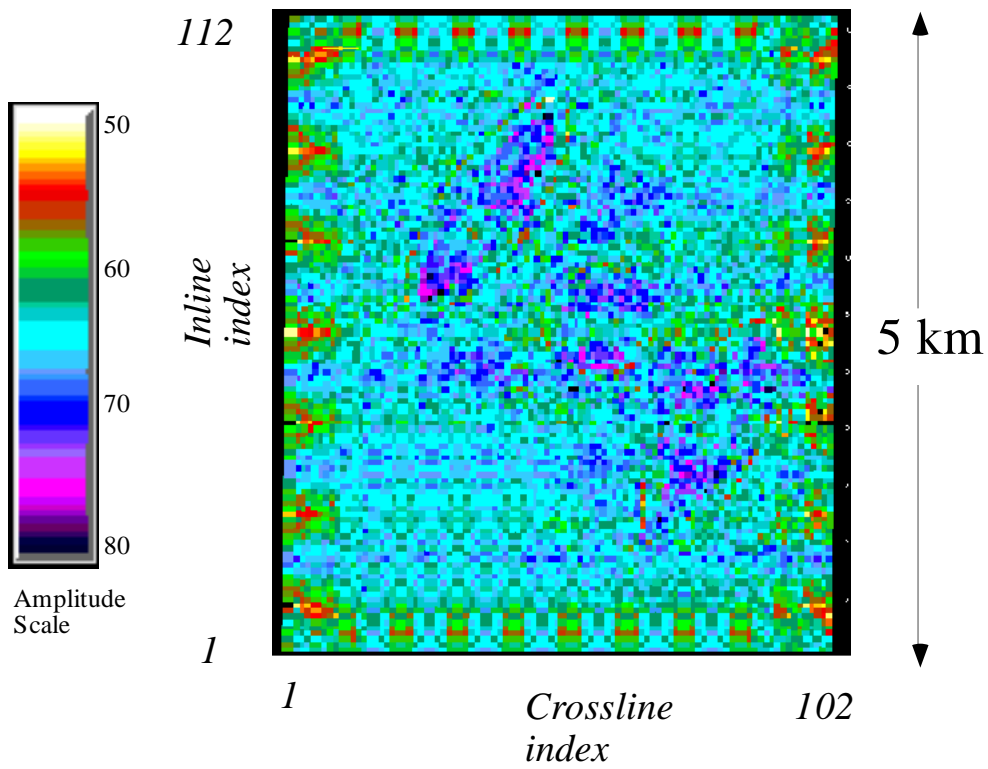


Figure 20: Viking P-P amplitude map: Clastic model.

From this example, the value of S-waves in imaging the clastic model is high. The exclusive use of acoustic seismic data would not be capable of unambiguously imaging the sand bodies. Detection of small changes in V_p/V_s in a map view with the power of 3-D pattern recognition can reveal subtler features than a 2-D profile can. The inclusion of shear data volumes for this isotropic model has doubled the amount of interpretable data and has enhanced the interpretation. It has also added confidence to the interpretation.

Carbonate model interpretation

The Landmark Seisworks® interpretation system is used to pick three horizons on the P-P and the P-S volumes of the carbonate model. The event correlations of Inline 44 for the P-P and P-S migrated volumes are shown in Figures 21 and 22, respectively. The broad bandwidth of the P-P data resolves the porosity base of the reef. The reef-to-basin transition is found at the disappearance of the lower porosity peak and its replacement by a weaker peak, which defines the top of the basin fill. The base of porosity and the top of the basin fill is combined into one horizon pick (the 'carbonate'). The map of the P-P amplitude of the carbonate marker (Figure 23) defines the reef edge along the black band running from northwest to northeast. It is also defined by the P-S amplitudes of the carbonate (Figure 24) and the Ireton (Figure 25). The shear section has a lower bandwidth, which is anticipated at this depth (Miller et al., 1994).

Despite its lower bandwidth, the shear amplitudes of the Nisku and the Ireton also define the reef edge. The P-S interpretation, which supplements the already established P-P interpretation, infers lithology based upon the V_p/V_s ratios calculated between the Wabamun and the Ireton markers (Figure 25). The calculated V_p/V_s values match the model for this interval. Figure 25 also reveals a decrease in the V_p/V_s ratio along the reef flank toward the northwest. This zone marks an increase in porosity due to the porosity wedge of the model. The P-P data clearly images the reef -to- basin transition, but the inclusion of shear data provides additional lithologic information that otherwise could not have been determined. The P-S information provides a powerful supplement to the acoustic interpretation and further characterizes the anomaly.

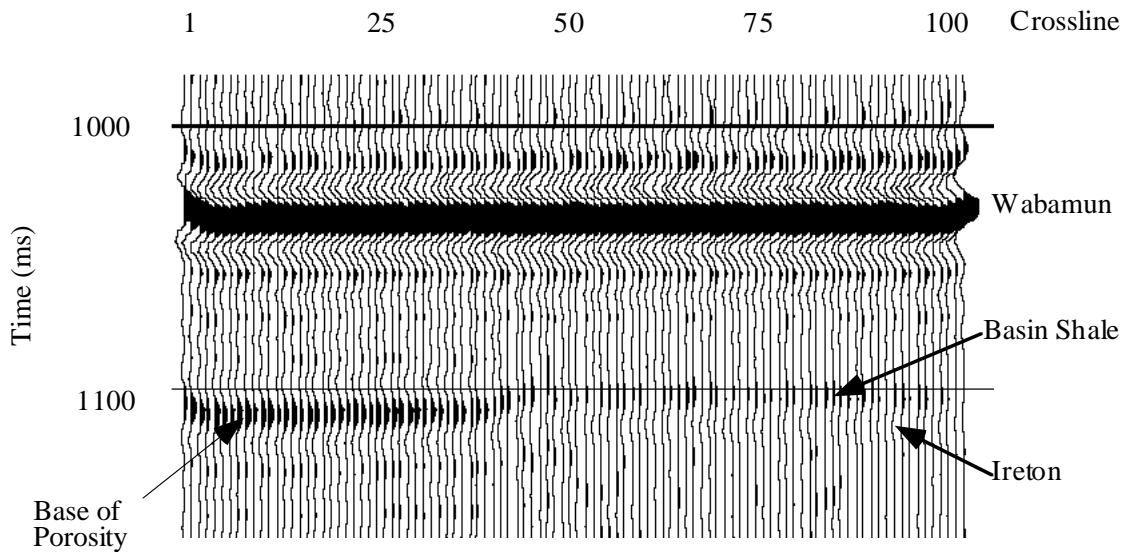


Figure 21: Inline 44 of the carbonate model: P-P migrated volume.

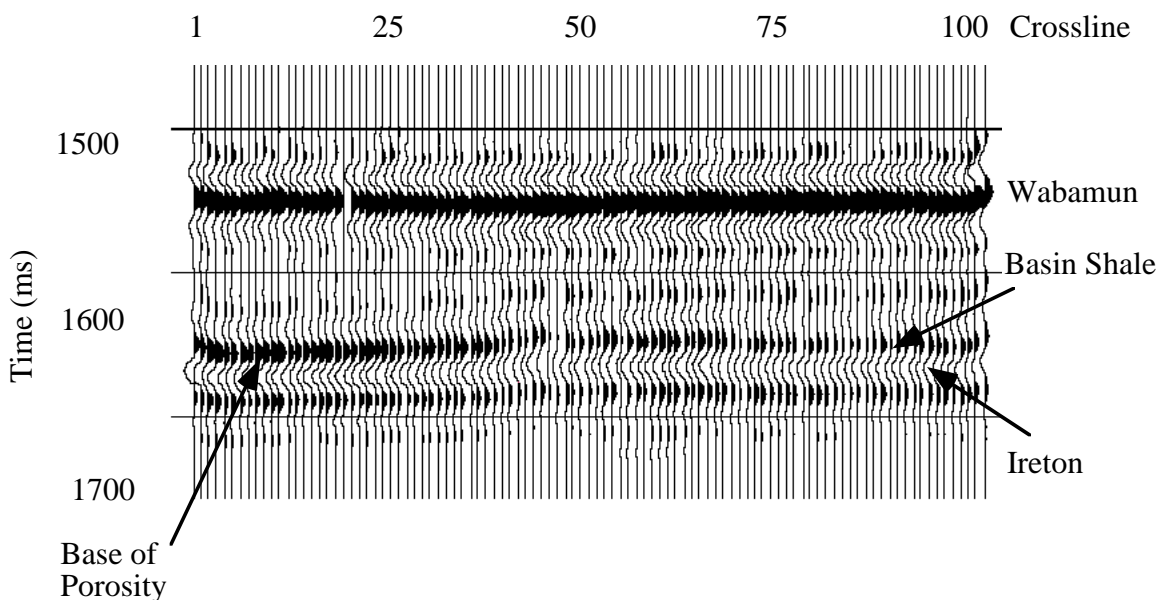


Figure 22: Inline 44 of the carbonate model: P-S migrated volume.

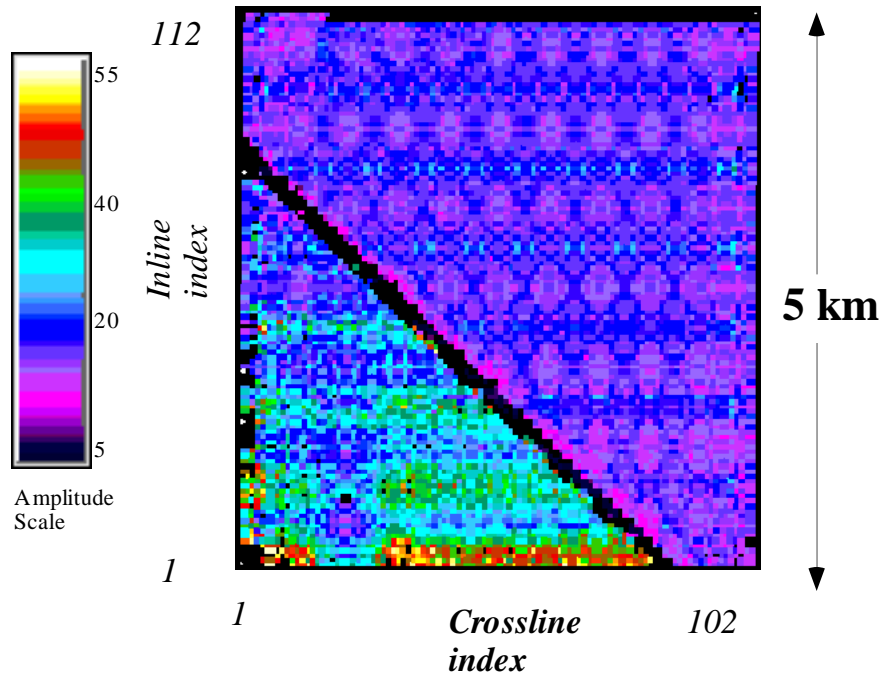


Figure 23: P-P carbonate amplitude map. Carbonate model.

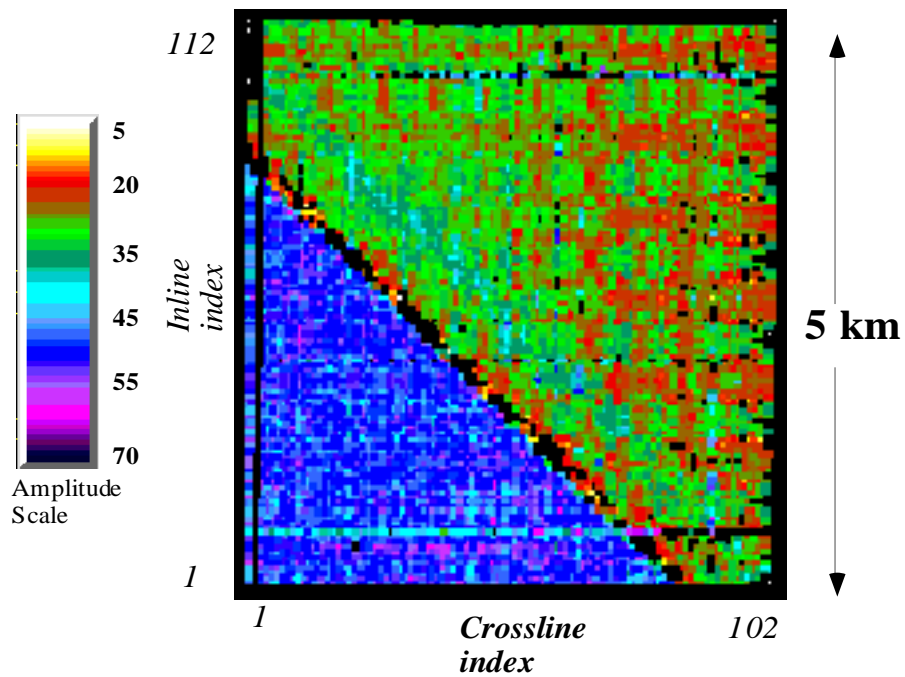


Figure 24: P-S carbonate amplitude map. Carbonate model.

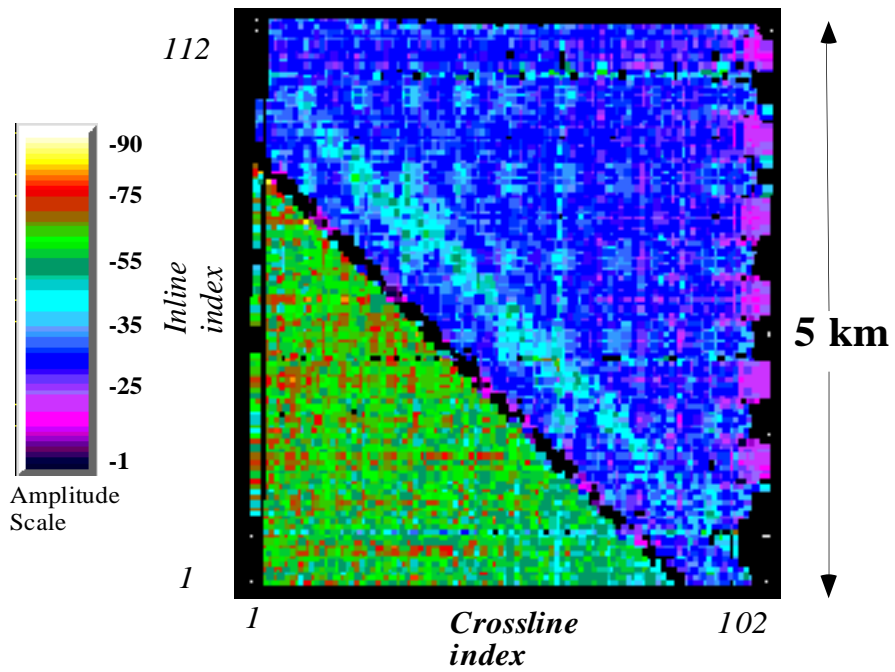


Figure 25: P-S Ireton amplitude map. Carbonate model.

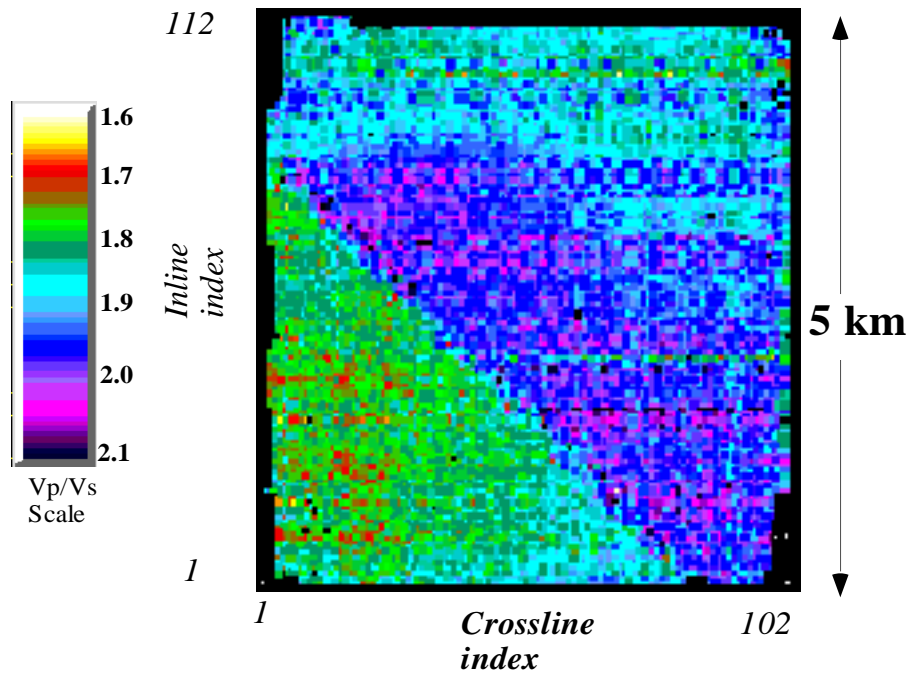


Figure 26: Vp/Vs (Wabamun to Ireton interval) map. Carbonate model.

TUNING EFFECTS UPON VP/VS RATIO CALCULATIONS

The V_p/V_s values for the BFS-to-Mannville interval of the clastic model are lower than the modelled values. Wavelet tuning effects may be partially responsible for this underestimation. The V_p/V_s calculations are based upon the interpreted time structures of the BFS and Mannville, and they may be affected by wavelet tuning within the Joli Fou shale.

A converted-wave 2-D seismic line is acquired over the clastic model in the orientation of cross-section A-A' in Figure 1 to test the effect of wavelet tuning upon calculated values of V_p/V_s . The line is acquired with an RI of 100m and SI of 300m. The processing procedures are a 2-D version of the 3-D processing flow described earlier. The P-S data are convolved with a 50 Hertz Ricker wavelet; the P-P data with a 60 Hertz Ricker. The Viking and Mannville horizons are interpreted on the P-P and P-S sections for a series of filtered-down versions of data. The V_p/V_s values are calculated for the Viking-to-Mannville isochrons along portions of the line where the Viking sand is not present (Figure 27). Within this zone is a 50m interval of Viking and Joli Fou shales with a modelled V_p/V_s of 2.05.

At 50 Hertz, the P-S section (Figure 27) clearly resolves the 30m Viking and the 20m Joli Fou shales. At 60 Hertz, the P-P data (Figure 28) does not resolve the Joli Fou shale. For given frequency and velocity, the wavelength is (Sheriff and Geldhart, 1982):

$$\lambda = \frac{V}{F}, \quad (5)$$

where F = the dominant frequency

V = the velocity

λ = the wavelength.

For a V_p/V_s ratio of 2.05,

$$\lambda_s = \frac{\lambda_p}{2}, \quad (6)$$

where λ_s = P-S wavelength

λ_p = P-P wavelength.

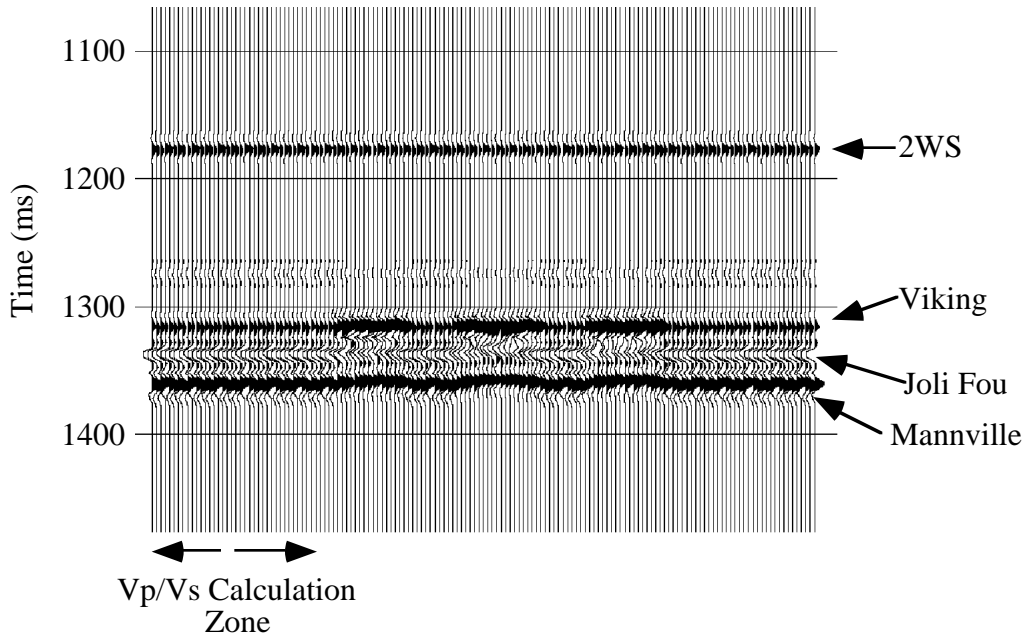


Figure 27: 2-D P-S migrated section of the clastic model. Dominant frequency = 50 Hz.

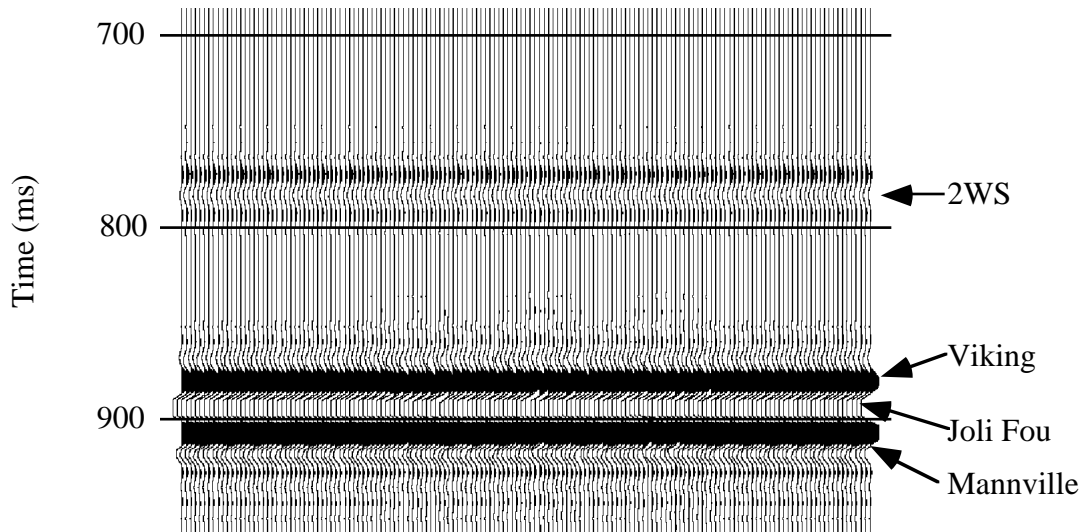


Figure 28: 2-D P-P migrated section of the clastic model. Dominant frequency = 60 Hz.

Equation (6) shows that the P-S and the P-P data will not have the same wavelengths and thus there will be not be consistent tuning effects for the same dominant frequency. This discrepancy will affect the horizon interpretations from the P-P and P-S datasets and will directly affect the V_p/V_s ratio calculations.

Table 4 summarizes the I_p , I_s , and the calculated V_p/V_s ratios for increasingly bandlimited data. The V_p/V_s ratio (Figure 29) decreases rapidly as the dominant frequency is reduced. The P-S Viking to Mannville interval (I_s) decreases data while the P-P interval (I_p) value *increases* as the frequency is reduced. The calculated V_p/V_s ratio for the Mannville to Viking interval is underestimated for frequencies below 50 Hz. due to wavelet tuning.

Dominant Frequency	I_p	I_s	V_p/V_s
50	27	44	2.20
40	29	38	1.6
30	29	38	1.6
20	35	39	1.2
15	48	50	1.08

Table 4: I_p , I_s , and V_p/V_s values for the Viking to Mannville interval for decreasing values of the dominant frequency

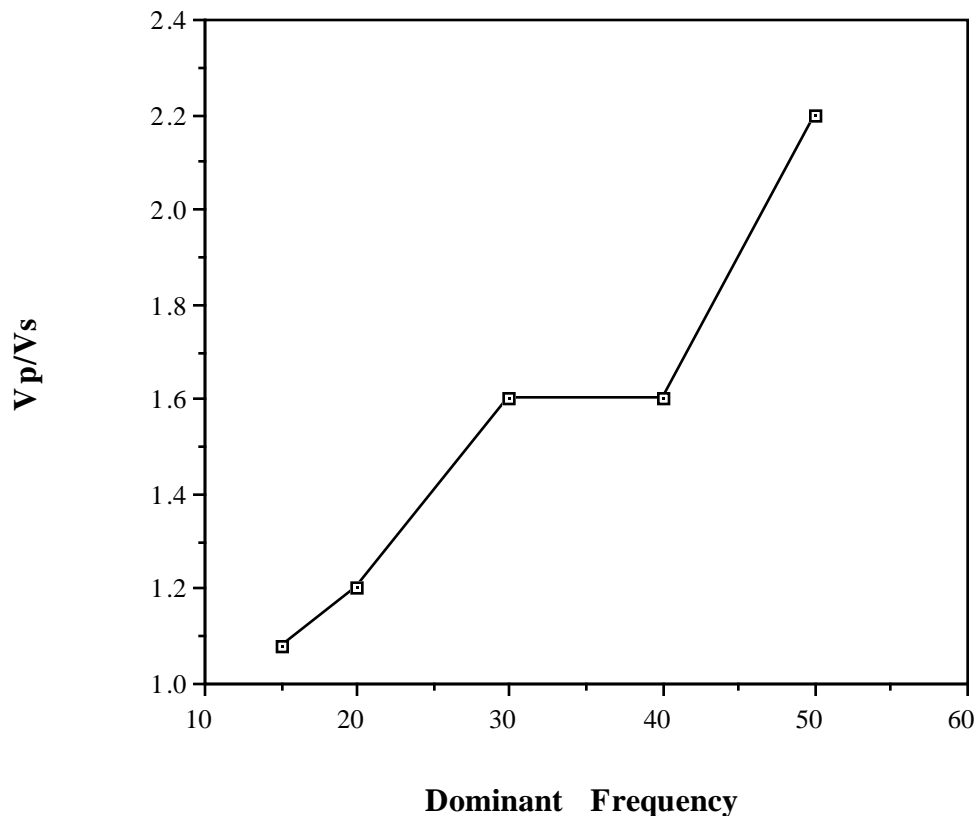


Figure 29: V_p/V_s versus P-P and P-S section dominant frequency. Clastic numerical model.

Dominant Frequency	Ip	Is	Vp/Vs
50	29	44	2.03
40	29	38	1.6
30	29	38	1.6
20	29	39	1.7
15	29	50	2.4

Table 5: Vp/Vs, Ip, and Is values for the Viking to Mannville interval for decreasing P-S dominant frequency. P-P dominant frequency = 40 Hz.

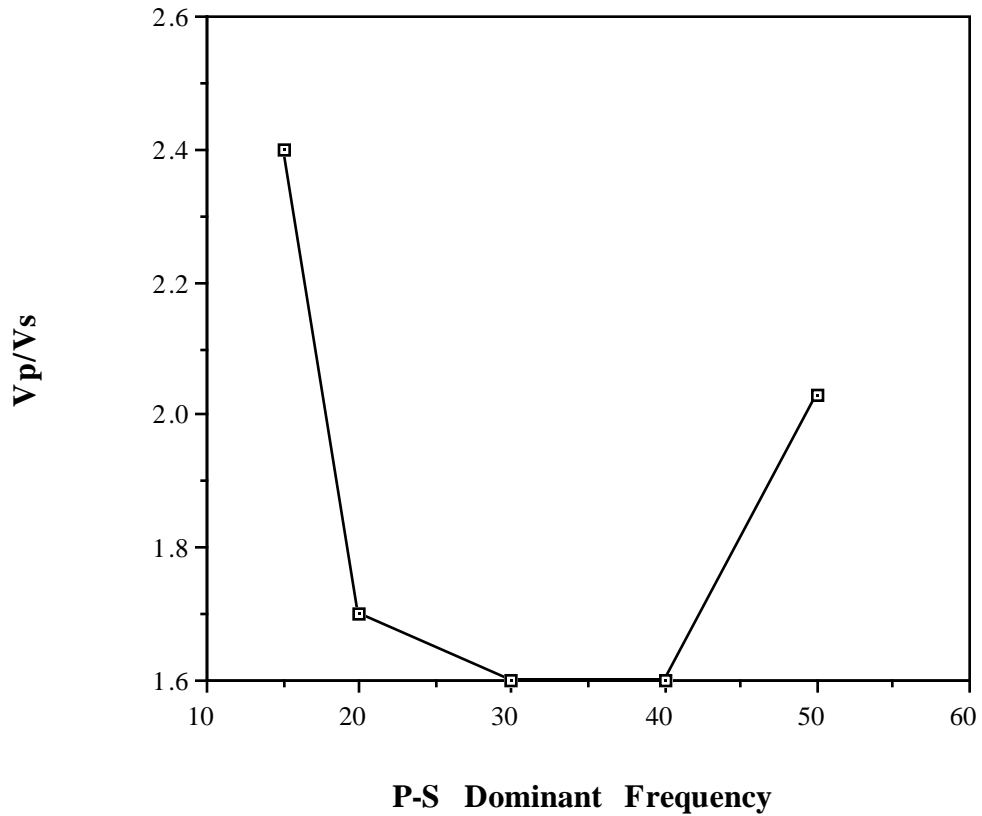


Figure 30: Vp/Vs versus P-S frequency. P-P frequency = 40 Hz. Clastic numerical model.

Figure 30 displays the calculated V_p/V_s versus the dominant frequency of the P-S wavelet for a constant P-P frequency of 40 Hz. As the P-S frequency decreases, the V_p/V_s ratio is underestimated by 20% in the 20 to 40 Hertz range, but is overestimated for very low frequencies. Tatham and McCormack (1989) recommend narrow intervals to calculate V_p/V_s ratios, but for low frequencies, these calculations may be compromised by tuning. Wavelet effects in V_p/V_s ratio calculations have been noted by Miller et al. (1994). Wavelet tuning has a serious effect upon the absolute value of the V_p/V_s ratio, but the relative changes of V_p/V_s should remain intact, if the wavelet is consistent throughout both datasets.

CONCLUSIONS

The two isotropic models show that the use of 3-D P-S data provides supplementary information to the acoustic 3-D survey. In the sand model, the shear is indispensable in delineating the Viking sands. In the reef model, the P-P data can adequately image the reef-to-basin transition. Comparative time intervals between the P-P and the P-S data result in V_p/V_s maps that can provide lithologic and thickness indicators. Combining this information in a 3-D measurement with the acoustic survey provides a more detailed interpretation; one which could not be achieved with acoustic data exclusively.

Differences in wavelet tuning between the P-P and the P-S wavelets may alter the absolute value of the V_p/V_s ratio maps. The relative difference, however, should remain intact and allow consistent mapping.

ACKNOWLEDGMENTS

Landmark Graphics Corporation generously donated their Seisworks3D interpretation software and the ProMax3D processing system. Western Geophysical, Inc. is thanked for its MIMIC modelling system donation. Shaowu Wang provided useful processing discussion and assistance. Sue Miller gave insightful suggestions on converted-wave interpretation.

REFERENCES

- Al-Bastaki, A.R., Arestad, J.F., Bard, K., Mattocks, B., Rolla, M.R., Sarmiento, V., Windells, R., 1994, Progress report on the characterization of Nisku carbonate reservoirs: Joffre field, south-central Alberta, Canada, *in*: Reservoir characterization project - phase 5 report, Colorado School of Mines.
- Brown, A.R., 1991, Interpretation of three-dimensional seismic data: AAPG Memoir 42, American Association of Petroleum Geologists.
- Cary, P.W., 1994, 3-D converted-wave seismic processing: CREWES Research Report, **6**, 31-1 - 31-10.
- Harrison, M.P., 1992, Processing of P-SV surface-seismic data: anisotropy analysis, dip moveout, and migration: PhD. dissertation, The University of Calgary.
- Harrison, M., and Stewart, R.R., 1993, Poststack migration of P-SV seismic data: *Geophysics*, **58**, 1127-1135.
- Lawton, D.C., 1994, Acquisition design of 3-D converted-waves: CREWES Research Report, **6**, 23-1 - 23-23.
- Lawton, D.C., Stewart, R.R., Cordsen, A., and Hrycak, S., Advances in 3C-3D design for converted-waves: CREWES Research Report, **7**, *this volume*.

- Leckie, D.A., Bhattacharya, J.P., Bloch, J., Gilboy, C.F., Norris, B, 1994. Cretaceous Colorado/Alberta group. In: Geological Atlas of the Western Canada Sedimentary Basin. G.D. Mossop and I. Shetson (comps.). Calgary, Canadian Society of Petroleum Geologists and Alberta Research Council, chpt. 20.
- Miller, S.L.M, Harrison, M.P., Lawton, D.C., Stewart, R.R., and Szata, K.J., 1994, Analysis of P-P and P-SV seismic data from Lousana, Alberta: CREWES Research Report, 6, 7-1 - 7-24.
- Nazar, B.D., 1991, An interpretive study of multicomponent seismic data from the Carrot Creek area of west-central Alberta: M.Sc. thesis, The University of Calgary.
- Schaffer, A., 1993, Binning, static correction, and interpretation of P-SV surface-seismic data: M.Sc. thesis, The University of Calgary.
- Sherrif, R.E., 1991, Dictionary of geophysical terms, SEG.
- Sheriff, R.E., and Geldart, L.P., 1982, Exploration Seismology, vol.1. Cambridge University Press.
- Slotboom, R.T., 1990, Converted-wave (P-SV) moveout estimation: 60th Ann. Internat. Mtg. Soc. Expl. Geophys., Expanded Abstracts, 1104-1106.
- Tatham, R.H. and McCormack, M.D., 1991, Multicomponent seismology in petroleum exploration: Investigations in geophysics - 6, Society of Exploration Geophysicists.